

## Magnetic susceptibility and ESR study of the covalent-chain antiferromagnets $\text{TlFeS}_2$ and $\text{TlFeSe}_2$

Z. Seidov,<sup>1,2</sup> H.-A. Krug von Nidda,<sup>1</sup> J. Hemberger,<sup>1</sup> A. Loidl,<sup>1</sup> G. Sultanov,<sup>2</sup> E. Kerimova,<sup>2</sup> and A. Panfilov<sup>3</sup>

<sup>1</sup>*Experimentalphysik V, Elektronische Korrelationen und Magnetismus, Institut für Physik, Universität Augsburg, D-86135 Augsburg, Germany*

<sup>2</sup>*Institute of Physics, Academy of Sciences of Azerbaijan, 370143 Baku, Azerbaijan*

<sup>3</sup>*B. Verkin Institute for Low Temperature Physics and Engineering, 47 Lenin Avenue, 310164 Kharkov, Ukraine*

(Received 20 April 2001; revised manuscript received 23 July 2001; published 13 December 2001)

We report on magnetic susceptibility, magnetization, electric resistivity, and ESR experiments on single crystals of the covalent-chain antiferromagnetic compounds  $\text{TlFeX}_2$  ( $X = \text{S}, \text{Se}$ ). Collinear magnetic order with strongly reduced moments sets in at  $T_N = 196$  K for  $\text{TlFeS}_2$  and at  $T_N = 290$  K for  $\text{TlFeSe}_2$ , respectively. The magnetic moments are oriented perpendicular to the chain direction. The temperature dependence of the electric resistivity reveals semiconducting behavior for both compounds. However, high-temperature susceptibility and ESR measurements strongly suggest a one-dimensional metallic character.

DOI: 10.1103/PhysRevB.65.014433

PACS number(s): 76.30.-v, 72.80.-r, 73.90.+f

### I. INTRODUCTION

The magnetic properties of thallium-thioferrate are dominated by chains of edge-linked  $\text{FeS}_4$  tetrahedra and hence reveal an almost one-dimensional (1D) character.  $\text{TlFeS}_2$  was originally described as a mineral ragunit by Laurent *et al.*<sup>1</sup> and was later synthesized by Klepp and Boller<sup>2</sup> and by Zabel and Range.<sup>3</sup> The crystal structure is monoclinic with space group  $C2/m$ , with lattice parameters  $a = 1.164$  nm,  $b = 0.531$  nm,  $c = 1.051$  nm, and  $\beta = 144.6^\circ$ .<sup>3</sup> Alternatively, in a nonstandard  $I112/m$  representation, which we will use throughout this paper, the lattice parameters read as  $a = 0.683$  nm,  $b = 1.051$  nm,  $c = 0.531$  nm, and  $\gamma = 98.6^\circ$ .<sup>3</sup> Note that  $b$  and  $c$  are interchanged with respect to the  $C2/m$  representation. For the  $I112/m$  representation the  $\text{FeS}_4$  tetrahedra build infinite chains along the  $c$  axis. The chains exhibit relatively short Fe-Fe distances, exceeding the Fe-Fe distance in metallic iron only by less than 10%. Hence, a certain degree of itinerancy along the chains and concomitant one-dimensional metallic behavior can be expected. The chains are linked together by the larger thallium ions and form roughly a triangular lattice. While the iron ions along the chains, in addition to a direct Fe-Fe exchange, are coupled via a Fe-S-Fe superexchange, the interchain coupling is mediated via Fe-S-Tl-S-Fe superexchange and certainly is much weaker. Minor structural differences and concomitant different interchain couplings distinguish thallium-thioferrate from the better known alkali-thioferrates  $A\text{FeS}_2$  ( $A = \text{K}, \text{Rb}, \text{Cs}$ ) (see references in Ref. 3, Tiwary and Vasudevan,<sup>4</sup> Welz *et al.*,<sup>5,6</sup> and Bronger and Müller<sup>7</sup>). Inelastic neutron-scattering results on  $\text{TlFeS}_2$  have been reported by Welz and Nishi<sup>8</sup> and by Welz *et al.*<sup>9</sup> From a detailed analysis of the magnon excitations the intrachain coupling has been determined as  $J = -55$  meV, while the interchain coupling in the almost regular triangular lattice amounts to  $(J_1 + J_2)/2 = -0.29$  meV and  $J_3 = 0.13$  meV. The weak interchain exchange gives rise to 3D long-range magnetic order below  $T_N = 196$  K.<sup>5</sup>

From a structural point of view, thallium-selenoferrate is

closely related to thallium-thioferrate [ $C2/m$ ;  $a = 1.197$  nm,  $b = 0.549$  nm,  $c = 0.711$  nm, and  $\beta = 118^\circ$  (Ref. 2)] but has been much less investigated. (For comparison the analogous values for  $c$  and  $\beta$  in  $\text{TlFeS}_2$  have to be recalculated as  $c = 0.672$  nm and  $\beta = 114^\circ$ , because different authors chose different lattice vectors for the monoclinic unit cell.) Heat capacity, magnetic susceptibility,<sup>10</sup> and Mössbauer spectroscopy in polycrystalline samples of  $\text{TlFeSe}_2$  (Refs. 11 and 12) have been reported revealing the one-dimensional magnetic character like in  $\text{TlFeS}_2$ .

These chain compounds are interesting because of a number of reasons.

(i) In these alloys Fe has nominally a valence of  $3+$ , with a half-filled  $d$  shell with no spin-orbit coupling. Hence, it is a half-integer spin system and gapless excitations can be expected. The spin value  $S = 5/2$  is large, and a classical spin model should be applicable. E.g., the spin dynamics of tetramethyl-ammonium manganese-chloride (TMMC) have been well described within classical limits.<sup>13,14</sup> However, covalence bonds<sup>3</sup> and partly the itinerancy of the Fe  $d$  electrons seem to reduce the spin value significantly.

(ii) The chains form an almost regular triangular lattice, yielding frustration effects in the interchain coupling. Slight changes of the monoclinic angle  $\beta$  can remove the magnetic interchain frustration and induce long-range 3D magnetic order.

(iii) The small Fe-Fe intrachain separation gives rise to strong covalence effects and is expected to promote charge-carrier delocalization. This effect should be especially dominant in the sulfur compound, which reveals the shortest Fe-Fe distance of 0.265 nm in these systems.

In this article we present detailed magnetic susceptibility, magnetization, electrical resistivity, and electron-spin-resonance (ESR) experiments on single-crystalline  $\text{TlFeS}_2$  and  $\text{TlFeSe}_2$ .

### II. EXPERIMENTAL DETAILS

Single crystals of  $\text{TlFeX}_2$  ( $X = \text{S}, \text{Se}$ ) were grown by the Bridgman method from powder obtained by silica-tube

synthesis.<sup>2,3,15</sup> The melting point was roughly located at 600 °C and 500 °C for TlFeS<sub>2</sub> and TlFeSe<sub>2</sub>, respectively. The needlelike shape of the crystals indicates the one dimensionality of the structure. The constituent fibers are strong, but they bend and can be separated easily. Fresh surfaces have a silver-metallic appearance. X-ray diffraction patterns were taken by means of a Guinier camera using Cu  $K\alpha$  radiation. No impurity phases have been detected. At room temperature, x-ray diffraction measurements confirmed the  $C2/m$  monoclinic structure for TlFeS<sub>2</sub> and TlFeSe<sub>2</sub>.

A commercial superconducting quantum interference device (SQUID) magnetometer from Quantum Design and a home-built Faraday balance were used to determine the susceptibility and magnetization of the samples within a temperature range  $1.5 \leq T \leq 400$  K. For technical reasons, the SQUID measurements of the single crystals were only performed with the magnetic field applied parallel to the chain direction. Nevertheless, the Faraday balance allowed us to determine the complete orientation dependence. The dc electrical resistivity has been measured with a standard four-probe technique for temperatures  $100 \leq T \leq 600$  K. ESR detects the power absorption  $P_{\text{abs}}$  of the samples from a magnetic microwave field  $h$  with frequency  $\omega = 2\pi\nu$  as a function of the static magnetic field  $H$  applied perpendicular to the microwave field. The ESR measurements were performed in a Bruker ELEXSYS 500 CW spectrometer working at X-band frequencies ( $\nu \approx 9.34$  GHz) within a temperature range  $100 \leq T \leq 550$  K using a nitrogen gas-flow cryostat (Bruker). To improve the signal-to-noise ratio, one records the field derivative of the absorption  $dP_{\text{abs}}/dH$  by the lock-in technique.

### III. EXPERIMENTAL RESULTS

#### A. Magnetic susceptibility and magnetization

The magnetic susceptibilities of TlFeS<sub>2</sub> and TlFeSe<sub>2</sub> are shown in Fig. 1 as a function of temperature for the magnetic field applied both parallel and perpendicular to the chain direction. In these single crystals the chain axis, which corresponds to the crystallographic  $c$  axis ( $I112/m$  representation), is the long axis of the needle-shaped samples. The results have not been corrected for diamagnetism or paramagnetic van Vleck contributions. The data are in good agreement with those published by Welz and Nishi for TlFeS<sub>2</sub>,<sup>8</sup> but are extended to higher temperatures.

In both compounds the susceptibility exhibits typical features for one-dimensional magnetic systems undergoing a 3D antiferromagnetic (AFM) phase transition at  $T_N = 196$  K and 290 K for TlFeS<sub>2</sub> and TlFeSe<sub>2</sub>, respectively. Below the 3D magnetic ordering temperature, as in classical antiferromagnets, the susceptibility splits into parallel and perpendicular susceptibility components with the spin direction approximately along the crystallographic  $a$  axis. The inset in each frame illustrates the angular dependence of the susceptibility in detail. Below  $T_N$ ,  $\chi$  amounts values close to 2.5 emu/mol with the field perpendicular to the magnetic moment (parallel  $c$  axis) and values close to 0.5 emu/mol with the field parallel to the moment (parallel  $a$  axis). For temperatures  $T > T_N$  the susceptibility becomes almost isotropic, and the smooth in-

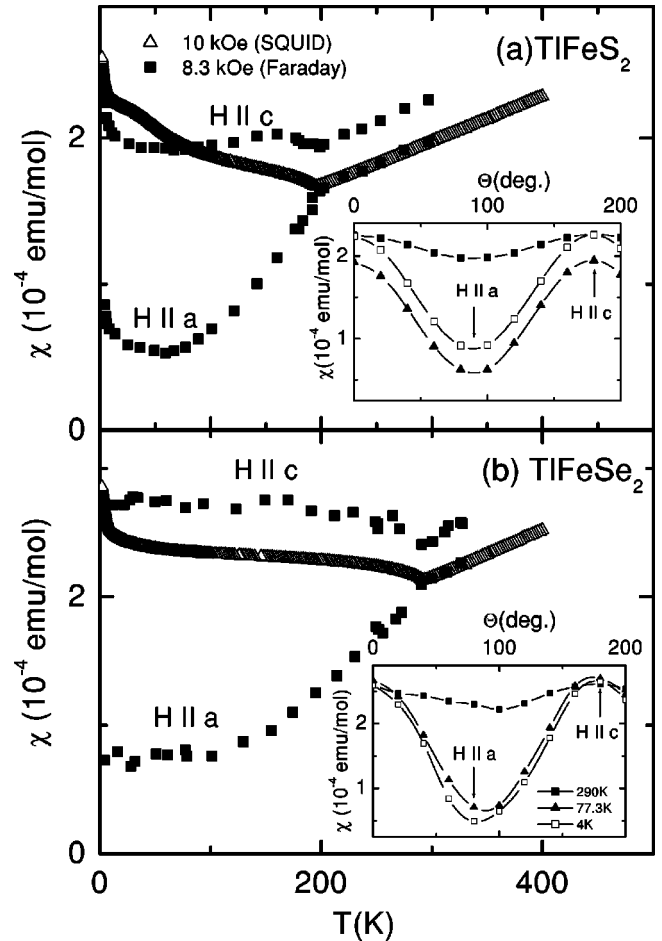


FIG. 1. Temperature dependence of the magnetic susceptibility in TlFeS<sub>2</sub> (a) and TlFeSe<sub>2</sub> (b) measured by Faraday balance for the magnetic field ( $H = 8.3$  kOe) applied parallel ( $\square$ ) and perpendicular ( $\blacksquare$ ) to the chain direction and by SQUID ( $\triangle$ :  $H = 10$  kOe,  $H \parallel$  chain). Insets: anisotropy of the susceptibility measured by the Faraday method at liquid-helium ( $\square$ ), liquid-nitrogen ( $\blacktriangle$ ), and room temperature ( $\blacksquare$ ), respectively.

crease on increasing temperature indicates the one-dimensional character for temperatures lower than the intrachain exchange interaction. However, the strictly linear increase of the susceptibility up to 400 K is rather unusual for one-dimensional spin chains, which typically exhibit a susceptibility maximum at a temperature comparable to the intrachain exchange. It seems that in this compound, via the strong and direct Fe-Fe exchange, a fraction of the  $d$  electrons is close to delocalization. This behavior will be discussed in more detail below.

The field dependence of the magnetization for TlFeS<sub>2</sub> and TlFeSe<sub>2</sub> is shown in Fig. 2. At all temperatures investigated, the magnetization increases almost linearly at  $H > 10$  kOe, as is characteristic for antiferromagnets, if the field is applied perpendicular to the easy axis, reaching values as low as  $0.001\mu_B$  for TlFeS<sub>2</sub> and  $0.002\mu_B$  for TlFeSe<sub>2</sub> at 50 kOe. The nonlinearity at low fields reveals a slight “ferromagnetic” component of about  $3 \times 10^{-4}\mu_B$ , which most probably results from a small nonzero amount ( $< 0.1\%$ ) of iron-defect states in domain walls. This ferromagnetic component also

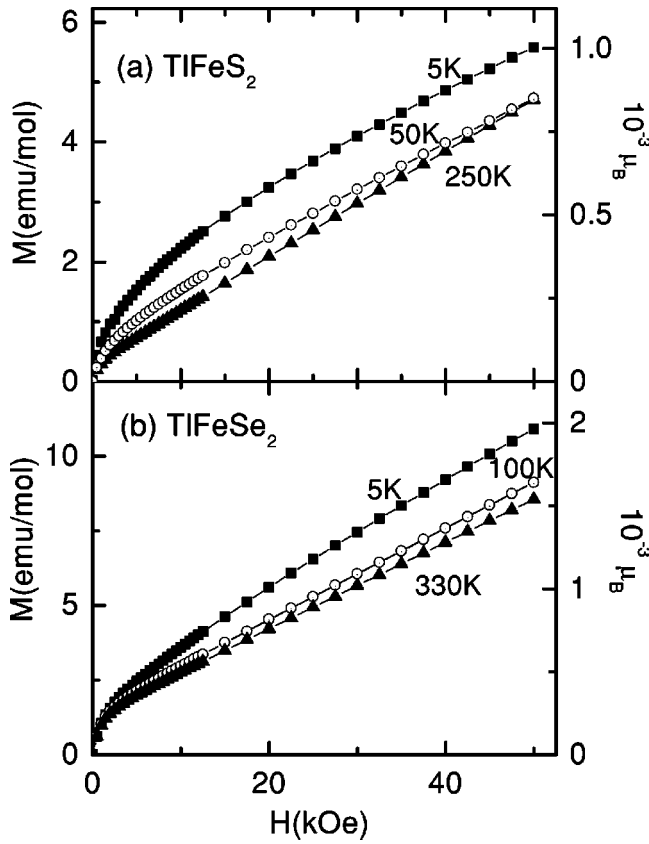


FIG. 2. Field dependence of the magnetization along the chain direction of  $\text{TlFeS}_2$  (a) and  $\text{TlFeSe}_2$  (b) at three different temperatures, two curves below and one above  $T_N$  for each compound.

explains the vertical shift, which exists between Faraday and SQUID measurements in Fig. 1. As the susceptibility was determined by  $\chi = M/H$ , the field-independent ferromagnetic component turns out to be stronger reduced at 10 kOe (SQUID) than at 8.3 kOe (Faraday).

### B. Electrical resistivity

The electrical resistance of both compounds has been investigated and is plotted in Fig. 3.  $\text{TlFeS}_2$  and  $\text{TlFeSe}_2$

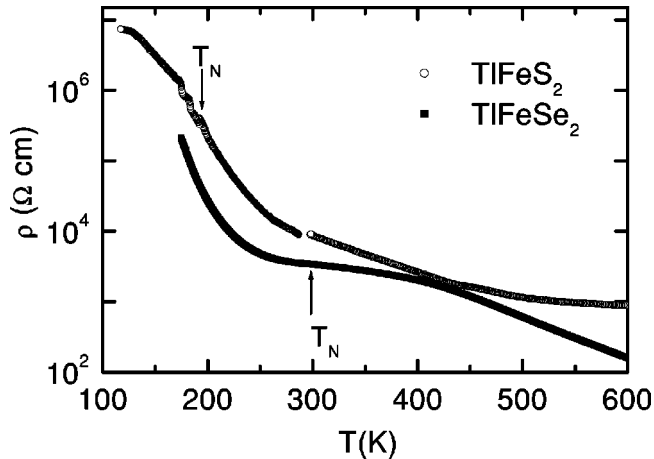


FIG. 3. Temperature dependence of the dc resistivity along the chain direction for single crystals of  $\text{TlFeS}_2$  and  $\text{TlFeSe}_2$ .

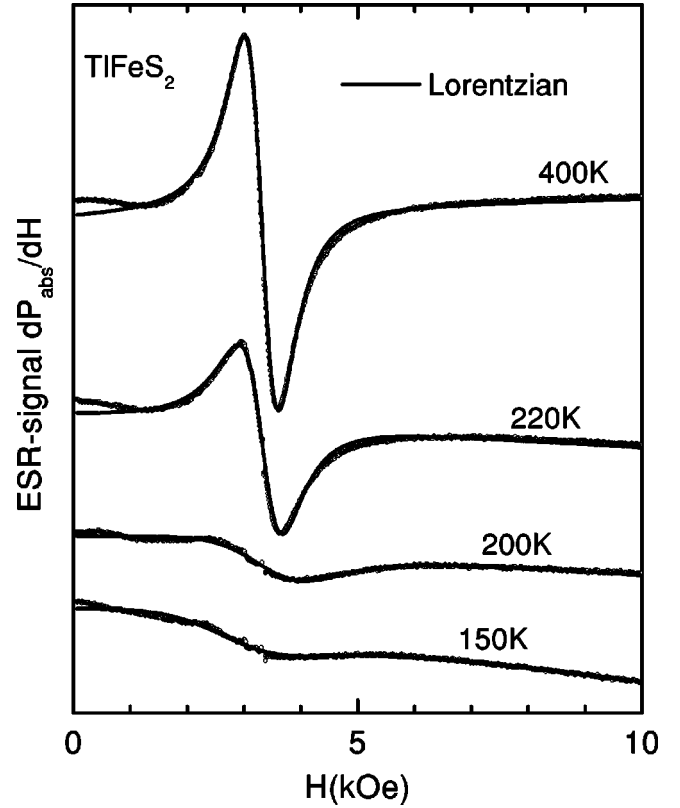


FIG. 4. ESR spectra of  $\text{TlFeS}_2$  at different temperatures. The solid line represents the fit curve following Eq. (1).

clearly reveal a semiconducting behavior, reaching values of  $10^6 \Omega \text{ cm}$  for the specific resistance along the chain direction at low temperatures. In sulfide the onset of 3D antiferromagnetic order close to 196 K is indicated by a small anomaly in the temperature-dependent resistance. Both compounds have been investigated up to temperatures of 600 K, but the character of the resistance always remains semiconducting ( $dp/dT < 0$ ).

### C. Electron-spin resonance

Figure 4 shows typical ESR signals of  $\text{TlFeS}_2$ : All samples under investigation reveal a well-defined but broad resonance absorption at resonance fields  $H_{\text{res}}$  near  $g = \hbar\omega/\mu_B H_{\text{res}} \approx 2$ . The signals are fitted by a single resonance line of Lorentzian shape (resonance field  $H_{\text{res}}$ , line-width  $\Delta H$ ) with a slight contribution of dispersion  $\alpha$ :

$$\frac{d}{dH} P_{\text{abs}} \propto \frac{d}{dH} \left( \frac{\Delta H + \alpha(H - H_{\text{res}})}{(H - H_{\text{res}})^2 + \Delta H^2} + \frac{\Delta H + \alpha(H + H_{\text{res}})}{(H + H_{\text{res}})^2 + \Delta H^2} \right). \quad (1)$$

Due to the large linewidth, we took into account both circular components at  $+H_{\text{res}}$  and  $-H_{\text{res}}$ , respectively. A nonzero dispersion-to-absorption ratio  $\alpha$  describes the asymmetry of the ESR line usually observed in metals, where the skin effect drives electric and magnetic microwave field out of phase.<sup>16,17</sup> But a nonzero  $\alpha$  is also a hint at the admixture of

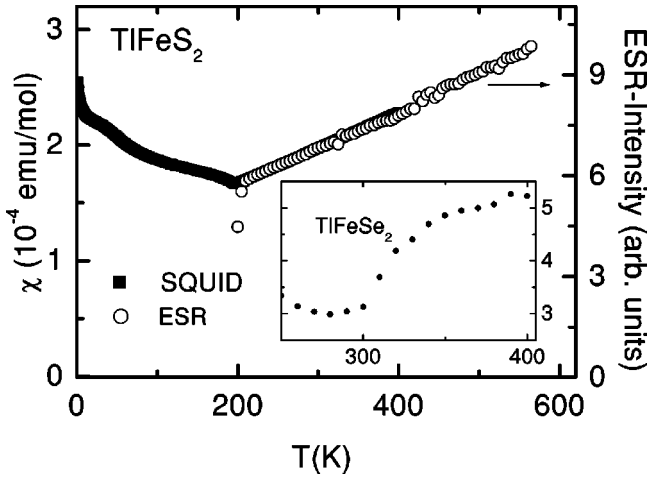


FIG. 5. Temperature dependence of the ESR intensity (right ordinate) in  $\text{TlFeS}_2$  compared to the static susceptibility (left ordinate). Inset: ESR intensity of  $\text{TlFeSe}_2$  (solid circles).

nondiagonal elements of the dynamic susceptibility to the signal, which is characteristic for linear-chain magnets.<sup>18</sup>

The fit curves describe the data quite well at temperatures  $T > T_N$ . Nevertheless, one observes deviations in the wings of the signal. At the Néel temperature, the resonance line strongly broadens and disappears due to the opening of the antiferromagnetic excitation gap, which has been determined for  $\text{TlFeS}_2$  by means of neutron scattering as  $\Delta \approx 4.5$  meV at 100 K.<sup>8</sup> However, an additional broad resonance line remains visible down to the lowest temperatures. The Lorentzian fit of the second signal is poor because of its strongly distorted shape. The existence of this second resonance line explains the observed deviations of the main resonance from a Lorentzian shape above the ordering temperature. Estimation of its intensity yields the same order of magnitude as the susceptibility measurements for  $H \parallel a$ , where the zero-temperature value is found to amount to about 1/3 of the susceptibility measured at  $T_N$ . Therefore we ascribe this part of the ESR spectrum to the same small amount of ferromagnetic iron defects, which may be also responsible for the residual magnetization observed in  $M(H)$  even at temperatures  $T > T_N$ .

Figure 5 shows the temperature dependence of the ESR intensity  $I_{\text{ESR}}$  of  $\text{TlFeS}_2$ , determined from the twofold integration of the field derivative of the Lorentzian line in comparison with the SQUID data of the static susceptibility. Above the Néel temperature, the intensity reveals an approximately linear increase from 220 K to 550 K with a relative slope comparable to that observed in the static susceptibility. As the ESR intensity is proportional to the spin susceptibility, this finding proves that all iron spins contribute to the ESR signal. In  $\text{TlFeSe}_2$  the linewidth at high temperatures  $T > T_N$  is about 4 times larger than in  $\text{TlFeS}_2$ . As it is nearly impossible to separate the main resonance from the parasitic spectrum of the iron impurities with a similar linewidth and intensity, we confine ourselves to the presentation of the ESR results of  $\text{TlFeS}_2$ . Nevertheless, as is shown in the inset of Fig. 5, a monotonous increase of the ESR inten-

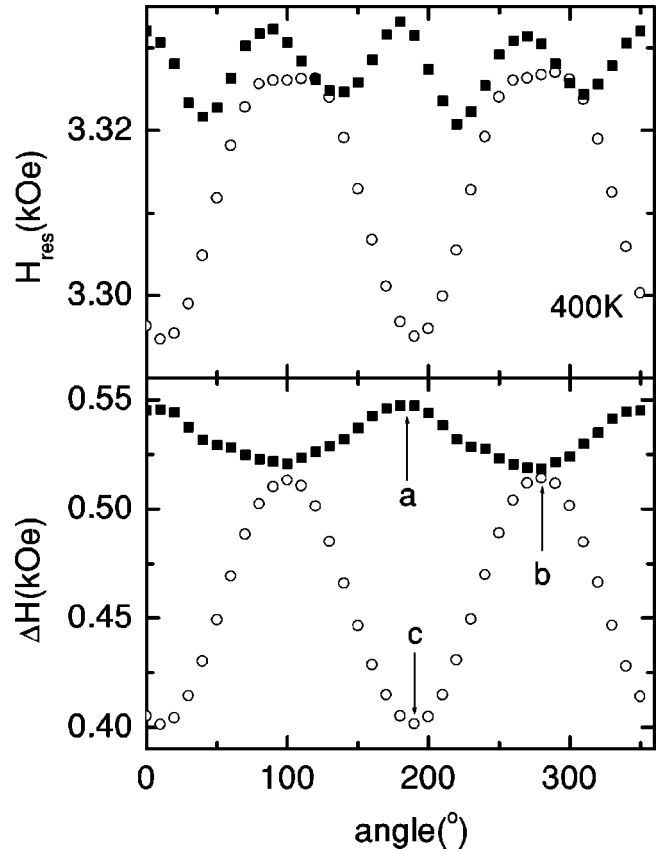


FIG. 6. Angular dependence of resonance field (upper frame) and linewidth (lower frame) in  $\text{TlFeS}_2$  for the magnetic field applied within the  $ab$  plane (solid squares) and  $bc$  plane (open circles) at  $T = 400$  K.

sity is observed with increasing temperature from 300 K to 400 K in agreement with the static susceptibility data.

Figure 6 shows the detailed anisotropy of resonance field (upper frame) and linewidth (lower frame) in  $\text{TlFeS}_2$  at 400 K for the static field  $H$  applied within both the  $ab$  plane and  $bc$  plane. Concerning the  $ab$  plane, the angular dependence of the resonance field exhibits a  $90^\circ$  periodic modulation with an amplitude of about 10 Oe due to the cubic crystal field acting on the Fe spins (nominally  $S = 5/2$ ) within the S tetrahedra. The linewidth follows a  $180^\circ$  symmetry, and the distance between the maximum and minimum of the linewidth amounts to about  $100^\circ$ , which directly reflects the geometry of the monoclinic lattice with an angle  $\gamma = 98.6^\circ$  between  $a$  and  $b$  axes. Regarding the  $bc$  plane, both the resonance field and linewidth show a  $180^\circ$  symmetry with a maximum in  $b$  and a minimum in  $c$  direction similar to  $\text{CsFeS}_2$ .<sup>19</sup> The amplitude of the anisotropy amounts about 30 Oe for the resonance field and 100 Oe for the linewidth. The anisotropy of the resonance field observed in the  $bc$  plane is in qualitative accordance with the weak anisotropy of the static susceptibility above  $T_N$ .

The full temperature dependences of the  $g$  value, asymmetry  $\alpha$ , and linewidth  $\Delta H$  are summarized in Fig. 7 for the magnetic field applied parallel to each of the three crystallographic axes in  $\text{TlFeS}_2$ : At high temperatures, the  $g$  value is almost temperature independent and close to 2.00 for  $H \perp c$ ,

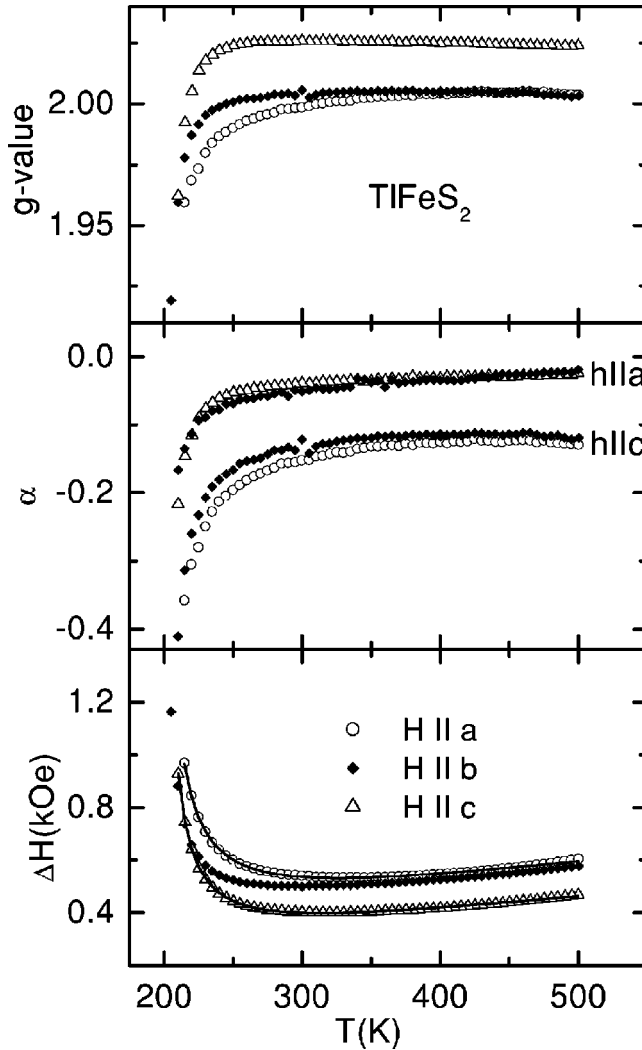


FIG. 7. Temperature dependence of the  $g$  value (upper frame), dispersion-to-absorption ratio  $\alpha$  for  $H\parallel b$  at two orientations of the incident microwave field  $h$  (middle frame), and linewidth (lower frame) in  $\text{TlFeS}_2$  for the magnetic field  $H$  applied parallel to the three crystallographic axes. The solid lines are fits due to Eq. (2).

indicating a spin-only value and an almost complete cancellation of orbital contributions, as is expected for a half-filled  $3d$  shell. For  $H\parallel c$ , one observes a slightly shifted  $g$  value of about 2.025, which also remains constant at high temperatures. The averaged  $g$  value  $g \approx 2.010$ , slightly above the free-electron value, is typical for  $\text{Fe}^{3+}$  tetrahedrally surrounded by sulfur ions and is in agreement with the values observed for  $\text{Fe}^{3+}$  in  $\text{ZnS}$  ( $g = 2.019$ ) (Ref. 20) and  $\text{KFeS}_2$  ( $g = 2.025$ ) (Ref. 21). These authors attribute the observed positive  $g$  shift to result from the covalency of the Fe-S bonds.

Approaching the Néel temperature from above, the resonance shifts to lower  $g$  values, indicating short-range order effects. The dispersion-to-absorption ratio  $\alpha$  shows a quite analogous behavior, starting at a nearly symmetric line shape at high temperatures and developing an increasing asymmetry near the ordering temperature. It is interesting to note that the asymmetry depends on the orientation of the incident

microwave field. The asymmetry is larger if the microwave field is applied parallel to the chain axis than if perpendicular. Such negative  $\alpha$  values have nothing to do with the skin effect but indicate the influence of the nondiagonal elements of the dynamic susceptibility in low-dimensional magnets as mentioned above.<sup>18</sup>

The linewidth exhibits a minimum value of 400 Oe (550 Oe) near room temperature for  $H\parallel c(a)$  and increases on increasing temperature with a slope of about 0.7 Oe/K. To lower temperatures the linewidth strongly increases and diverges at  $T = T_N$ . The full temperature dependence of the linewidth is well described by

$$\Delta H = \Delta H_0 + bT + \frac{C}{(T - T_N)^\delta}. \quad (2)$$

The critical exponent for the line broadening near  $T_N$  is found to be near  $\delta = 0.8$  comparable to  $\delta = 0.5$  in  $\text{KFeS}_2$ .<sup>22</sup> Such small critical exponents are often experimentally observed in low-dimensional magnets in contrast to theoretical expectations. This effect is ascribed to the increase of the staggered susceptibility due to three dimensional antiferromagnetic fluctuations on approaching the phase transition.<sup>23</sup>

#### IV. DISCUSSION AND CONCLUSION

The present single-crystal investigations of the  $\text{TlFeX}_2$  ( $X = \text{S}, \text{Se}$ ) covalent-chain antiferromagnets by SQUID, Faraday susceptibility, electric resistivity, and ESR measurements well confirm the quasi-1D properties and the occurrence of collinear 3D order with moments pointing perpendicular to the chains below  $T_N \approx 196$  K and  $T_N \approx 290$  K, respectively. In the following discussion we will try to give reasonable arguments that the TI compounds seem to be one-dimensional metals, although the resistance shows semiconducting behavior.

As mentioned above, the single-crystalline samples consist of thin fibers with a silver metallic gleaming. The crystals are difficult to treat, because they easily break into pieces. Hence, it is hard work to contact them for resistance measurements. To prove one-dimensional conductivity, it would be necessary to probe the current within the fibers. Due to the large separation of neighboring chains, a perpendicular current flow is impossible. However, defects and mechanical breaks in the chains are inevitable and therefore obviously dominate the conductivity, resulting in an increasing resistivity with decreasing temperature. This idea is in agreement with Nishioka *et al.*,<sup>24</sup> who predict the alkaline compound  $\text{KFeS}_2$  to be metallic on a microscopic scale despite macroscopic semiconducting behavior. For this reason, resistance measurements do not seem to be reliable and it is necessary to look carefully for hints on metallic behavior in the other measured properties.

Comparing the spin susceptibilities of  $\text{TlFeS}_2$  and  $\text{TlFeSe}_2$  obtained by SQUID and ESR measurements to that of the related alkaline compounds  $\text{AFeS}_2$  ( $A = \text{K}, \text{Cs}$ ), it turned out that they are quite similar in temperature dependence and magnitude (about  $2 \times 10^{-4}$  emu/mol at room temperature). However, the alkaline compounds reveal a sus-

TABLE I. Comparison of intrachain Fe-Fe distance  $d(\text{Fe-Fe})$ , ordered moment  $\mu_{\text{ord}}$ , susceptibility maximum  $T_{\text{max}}$ , and intrachain Heisenberg exchange  $J$  for  $S=3/2$  in  $A\text{FeS}_2$  ( $A=\text{K}, \text{Cs}, \text{Tl}$ ).

Compound	$d(\text{Fe-Fe})$ (nm)	$\mu_{\text{ord}}(\mu_{\text{B}})$	$T_{\text{max}}$ (K)	$J$ (meV)
KFeS <sub>2</sub>	0.270	2.43	565	-10
CsFeS <sub>2</sub>	0.271	1.88	800	-15
TlFeS <sub>2</sub>	0.265	1.85	1600	-29

ceptibility maximum, which is typical for one-dimensional antiferromagnetic Heisenberg chains, at  $T_{\text{max}}=565$  K for KFeS<sub>2</sub> and  $T_{\text{max}}=800$  K for CsFeS<sub>2</sub>, whereas the Tl compounds exhibit a continuous linear increase (up to 600 K for TlFeS<sub>2</sub>) and do not show any tendency for saturation. Welz and Nishi<sup>8</sup> estimated the position  $T_{\text{max}}$  of the susceptibility maximum for a Heisenberg chain,

$$\mathcal{H}_{1\text{D}} = -2J \sum_i \mathbf{S}_i \mathbf{S}_{i+1}, \quad (3)$$

using the exchange constant  $J$  obtained from neutron scattering for both a classical  $S=0.93$  spin chain with  $J=-55$  meV and a quantum spin chain with  $S=3/2$  for a renormalized  $J=-29$  meV. For the classical chain they calculated  $T_{\text{max}} \approx 0.95S^2|J|/k_{\text{B}} \approx 520$  K in comparison to  $T_{\text{max}} \approx 1600$  K for the quantum spin chain, where the maximum is approximately given by

$$T_{\text{max}} \approx 4.75|J|/k_{\text{B}}. \quad (4)$$

From our measurements up to 600 K, the first possibility can be ruled out, and a description of the high-temperature susceptibility ( $T > T_{\text{N}}$ ) in terms of a  $S=3/2$  quantum spin chain seems rather likely.

Tiwary and Vasudevan<sup>4</sup> analyzed the susceptibilities of the alkaline compounds within the model of a  $S=1/2$  spin chain. However, the ordered moments of the alkaline compounds found at low temperatures are slightly larger ( $2.43\mu_{\text{B}}$  for KFeS<sub>2</sub>) than or nearly comparable ( $1.88\mu_{\text{B}}$  for CsFeS<sub>2</sub>) to the ordered moment of  $1.85\mu_{\text{B}}$  in TlFeS<sub>2</sub>. For a  $S=1/2$  chain, the ordered moment is expected to amount to  $1\mu_{\text{B}}$ . Therefore, we suggest that the alkaline compounds have to be treated as  $S=3/2$  chains as well, which is in agreement with the work of Welz *et al.*<sup>5</sup> on KFeS<sub>2</sub>. Then the exchange constants can be estimated like in TlFeS<sub>2</sub> from the susceptibility maxima according to Eq. (4) as  $J=-10$  meV for KFeS<sub>2</sub> and  $J=-15$  meV for CsFeS<sub>2</sub>, respectively. Table I resumes the Heisenberg exchange  $J$  of the three sulfide compounds due to the model of a  $S=3/2$  antiferromagnetic spin chain together with the intrachain Fe-Fe distance. The reduction of the Fe-Fe distance by 2% from KFeS<sub>2</sub> to TlFeS<sub>2</sub> increases the exchange interaction by a factor of 3 and therefore indicates a strongly increasing degree of delocalization.

The increase of delocalization should also lead to the enhancement of the metallic character in the Tl compounds, making them one-dimensional metals.

Up to now, only a few works have been done in the field of  $S=3/2$  antiferromagnetic Heisenberg chains like, e.g., CsVCl<sub>3</sub>,<sup>25</sup> which are just at the borderline between quantum mechanical  $S=1/2$  chains and classical chains with large spins  $S \geq 5/2$ . By means of the density-matrix renormalization-group technique, Hallberg *et al.* have shown that the  $S=3/2$  chain belongs to the same universality class as the  $S=1/2$  Heisenberg chain.<sup>26</sup> From this point of view it should be sensible to compare the experimental results to analogous findings in  $S=1/2$  chains: A quite similar behavior has been observed in the series of organic linear-chain tetramethyl-tetrathia fulvalen (TMTTF)<sub>2</sub> $X$  and tetramethyl-tetraselena fulvalen (TMTSF)<sub>2</sub> $X$  compounds with, e.g.,  $X = \text{PF}_6, \text{AsF}_6, \text{and Br}$ .<sup>27</sup> The degree of delocalization of the charge carriers can be tuned by either hydrostatic pressure or chemical composition. The sulfur compound (TMTTF)<sub>2</sub>PF<sub>6</sub> shows charge localization and hence semiconducting behavior along the chains. Its susceptibility reveals a maximum near 300 K. In contrast, the selen compound (TMTSF)<sub>2</sub>PF<sub>6</sub> is a one-dimensional metal and its susceptibility increases monotonously within the accessible temperature range. Taking into account the delocalization of the electrons, the susceptibility was fitted satisfactorily with an exchange coupling  $|J|/k_{\text{B}}=700$  K. Hence, as in the case of alkaline and Tl compounds, the metallic behavior is accompanied by the increase of the exchange integral.

Unfortunately, it was not possible to describe the strong linear increase of the susceptibility in TlFeS<sub>2</sub> by the same fit like in (TMTSF)<sub>2</sub>PF<sub>6</sub> because that theory does not take into account the dimerization which is obviously present in TlFeS<sub>2</sub>. As we can see from comparison of the susceptibilities in KFeS<sub>2</sub> (undimerized) and CsFeS<sub>2</sub> (dimerized), the dimerization yields a clearly larger temperature variation below the susceptibility maximum with respect to the undimerized case. However, the dimerized chain is only treated for localized spins and strongly deviates from linear behavior. Hence TlFeS<sub>2</sub> is found between these cases of a dimerized chain with localized spins and an undimerized chain near delocalization.

In conclusion, we presented an experimental study of the quasi-one-dimensional antiferromagnetic chain compounds TlFeS<sub>2</sub> and TlFeSe<sub>2</sub> by means of susceptibility, resistivity, and electron-spin resonance. Both compounds reveal a semiconducting behavior in the resistivity measurements, whereas due to their magnetic properties, they seem to be one-dimensional metals. The main argument for metallic behavior is the temperature dependence of the magnetic susceptibility and ESR intensity, which both increase linearly from the Néel temperature up to the highest temperature (600 K) accessible in our measurements and do not show any tendency for saturation. Comparing this behavior to the one-dimensional organic (TMTTF)<sub>2</sub> $X$  and (TMTSF)<sub>2</sub> $X$  compounds, we argued that a shift of the characteristic antiferromagnetic spin-chain susceptibility maximum to very high temperatures is closely related to an increasing intrachain

exchange interaction and onset of one-dimensional metallic conductivity.

#### ACKNOWLEDGMENTS

We gratefully acknowledge D. Vieweg, M. Müller, and A. Pimenova for SQUID susceptibility and x-ray measurements

and V. N. Glazkov for useful discussions. This work was supported partly by Bundesministerium für Bildung und Forschung (BMBF) under the Contract No. EKM13N6917/0 and Deutsche Forschungsgemeinschaft (DFG) within Sonderforschungsbereich SFB 484 (Augsburg). Z.S. received financial support from Deutscher Akademischer Austauschdienst (DAAD).

- 
- <sup>1</sup>Y. Laurent, P. Picot, and R. Pierrot, *Bull. Soc. Fr. Mineral. Cristallogr.* **92**, 38 (1969).  
<sup>2</sup>K. Klepp and H. Boller, *Monatsh. Chem.* **110**, 1045 (1979).  
<sup>3</sup>M. Zabel and K.J. Range, *Z. Naturforsch. B* **34**, 1 (1979).  
<sup>4</sup>S. Tiwary and S. Vasudevan, *Phys. Rev. B* **56**, 7812 (1997).  
<sup>5</sup>D. Welz, M. Kohgi, Y. Endoh, M. Nishi, and M. Arai, *Phys. Rev. B* **45**, 12319 (1992).  
<sup>6</sup>D. Welz, M. Winkelmann, H.M. Mayer, and M. Nishi, *Physica B* **234-236**, 576 (1997).  
<sup>7</sup>W. Bronger and P. Müller, *J. Alloys Compd.* **246**, 27 (1997).  
<sup>8</sup>D. Welz and M. Nishi, *Phys. Rev. B* **45**, 9806 (1992).  
<sup>9</sup>D. Welz, S. Itoh, and A.D. Taylor, *Europhys. Lett.* **34**, 293 (1996).  
<sup>10</sup>M.A. Aldzhanov, N.G. Guseinov, G.D. Sultanov, and M.D. Nadzafzade, *Phys. Status Solidi B* **159**, K107 (1990).  
<sup>11</sup>R. Berger, L. Haggstrom, and T. Sundqvist, *Chem. Scr.* **28**, 47 (1988).  
<sup>12</sup>G.D. Sultanov, S.G. Ibragimov, A. Shukyurov, and M. Kasumov, *Fiz. Tverd. Tela* **29**, 2138 (1987) [*Sov. Phys. Solid State* **29**, 1229 (1987)].  
<sup>13</sup>M. Steiner, J. Villain, and C.G. Windsor, *Adv. Phys.* **25**, 87 (1976).  
<sup>14</sup>L.J. de Jongh and A.R. Miedema, *Adv. Phys.* **93**, 1 (1983).  
<sup>15</sup>D. Welz, P. Deppe, W. Schäfer, H. Sabrowsky, and M. Rosenberg, *J. Phys. Chem. Solids* **50**, 297 (1989).  
<sup>16</sup>G. Feher and A.F. Kip, *Phys. Rev.* **98**, 337 (1955).  
<sup>17</sup>F.J. Dyson, *Phys. Rev.* **98**, 349 (1955).  
<sup>18</sup>H. Benner, M. Brodehl, H. Seitz, and J. Wiese, *J. Phys. C* **16**, 6011 (1983).  
<sup>19</sup>Y. Matsuda, Y. Ito, and M. Nishi, *J. Phys. Soc. Jpn.* **53**, 2771 (1984).  
<sup>20</sup>H. Watanabe, *J. Phys. Chem. Solids* **25**, 1471 (1964).  
<sup>21</sup>W.V. Sweeney and R.E. Coffman, *Biochim. Biophys. Acta* **286**, 26 (1972).  
<sup>22</sup>R.S. de Biasi, C.A. Taft, and N.C. Furtadso, *J. Magn. Magn. Mater* **125**, 125 (1980).  
<sup>23</sup>H. Benner and J. Boucher, in *Magnetic Properties of Layered Transition Metal Compounds*, edited by L.J. de Jongh (Kluwer Academic, Dordrecht, 1990).  
<sup>24</sup>S. Nishioka, H. Kuriyaki, and H. Hirakawa, *Synth. Met.* **71**, 1877 (1995).  
<sup>25</sup>S. Itoh, Y. Endoh, K. Kakurai, and H. Tanaka, *Phys. Rev. Lett.* **74**, 2375 (1995).  
<sup>26</sup>K. Hallberg, X.Q.G. Wang, P. Horsch, and A. Moreo, *Phys. Rev. Lett.* **76**, 4955 (1996).  
<sup>27</sup>M. Dumm, A. Loidl, B.W. Fravel, K.P. Starkey, L.K. Montgomery, and M. Dressel, *Phys. Rev. B* **61**, 511 (2000).